 Polar Record 48 (247): 334–341 (2012). © *Cambridge University Press 2011. doi:10.1017/S0032247411000635*

Chemical analysis of ice vein μ-environments

Robert E. Barletta and Christopher H. Roe
Department of Chemistry, University of South Alabama, Mobile, AL 36688, USA
(rbarletta@southalabama.edu)

Received June 2011; First published online 23 November 2011

ABSTRACT. Icy environments (glacial ice and sea ice) can be complex ecosystems, supporting a diversity of communities. In particular, the μ-environments in which bacteria and algae are found are poorly understood. One important habitat is the liquid trapped in the ice, either as veins and triple junctions inherent in the ice structure or as liquid inclusions. μ-Raman spectroscopy is an analytical tool with the potential to characterise qualitatively and quantitatively these liquid μ-environments especially with respect to molecular anions such as nitrate, sulphate, bisulphate and MSA. Using a model system for glacial ice, splat-cooled samples were prepared from aqueous solutions of these anions at varying concentrations (50–75 mM total sulphate, 30–200 mM nitrate, and 10–55 mM MSA). Concentrations of these anions in the vein liquid were measured directly and non-destructively at –15 °C using μ-Raman spectroscopy. In agreement with predicted concentrations in glacial ice veins, it was found that typical ionic concentrations in veins are quite high, with mean concentrations ranging from 0.23 M to 3.5 M depending on anion type and initial concentration. For sulphate solutions, it was also possible to measure vein pH's directly. The observed pH in these systems was extremely low, in some cases ~1. The results of these model studies as well as the implications for ice vein concentrations in natural systems of polycrystalline ice are discussed.

Introduction

Icy environments (glacial ice and sea ice) can be complex ecosystems, supporting a diversity of communities. The production of these communities can, in fact, be quite large (Thomas 2002). In sea ice, for example, algal concentrations can reach those found in open ocean blooms (Stevens 1995). Initially, brine channels in the ice help to maintain contact with the open ocean. However, these channels can become closed off, leaving the biota in an isolated environment. In low porosity ices (<10%), the ice is cut off from the atmosphere and as the ice channels diminish in diameter, the environment can become increasingly isolated (Eichen 1992). Priscu and others (2007) have provided an overview of the biological diversity found in glacial environments. The effect that these extremophiles have on their local environment can be profound. For example, Christner (2010) points out that proteins produced by bacteria can affect the properties of the ice crystal surrounding them, much as antifreeze proteins of fish inhibit the growth of ice crystals to produce non-cryoscopic depression of the freezing point of water.

Despite the increasing interest in biological activity in ice, the μ-environments in which bacteria and algae are found are poorly understood. Price and others have proposed 3 basic habitats for microbes in ice and provided evidence for the ability of microbes to metabolise, albeit slowly, in each of them (Tung 2006; Rhode 2006, 2008; Price and others 2009). The three μ-environments proposed are: the liquid veins that exist between ice crystals, mineral grain surfaces; and the ice crystals themselves. In the first two, nutrients are supplied by the environment, while for ice crystals, the nutrient source consists of impurities diffusing through the crystal. Price and others characterise the state of uncertainty in the nature of the ice vein environment as follows, while leaving the exact nature of the chemical environment otherwise undiscussed: 'Depending on the composition of the ionic impurities in the vein and the amount by which the freezing point is depressed, the environment in the vein may require adaptation to a strongly acidic or caustic medium in addition to adaptation to low temperature' (Price and others 2009). It is, of course, well known that, as water freezes, impurities concentrate at the grain boundaries. Further, as the crystals themselves grow, impurities are further concentrated as the impurity front moves in a manner similar to the process of zone refining. The ice vein impurity concentrations have been estimated from bulk measurements of impurities in glacial ice by Mader and others (2006) and are listed in Table 1.

Table 1. Projected glacial ice vein concentrations at −10°C from Mader and others (2006).

Compound	Concentration (M)
Formic acid	0.69
Oxalic acid	0.017
Acetic acid	1.387
HSO_4^-	0.693
NO_3^-	2.080
$CH_3SO_3^-$ (MSA)	0.069
Total molarity, M	3.52

It is instructive to consider the physical chemistry controlling the process of keeping the material in the veins liquid. Using a simple colligative properties analysis, the mixture specified in Table 1 should not be liquid at −10°C. Rather, based on a simple freezing point depression analysis, it would freeze at −6.5°C. More generally, from the standpoint of cryoscopic calculations, much higher concentrations than those hypothesised would be expected in ice veins. For example an impurity molarity of >20 M would be necessary to depress the freezing

point of water to -40°C. From a thermodynamic perspective, the existence of liquid in ice at low temperatures may be readily understood from a consideration of binary phase diagrams between water and the constituent anions, particularly those of nitrate and sulphate, two anions of interest from an atmospheric chemistry perspective. Recent measurements of the binary phase diagrams of sulphate (Beyer 2003) and nitrate (Beyer and Hansen 2002) indicate the presence of low melting eutectic compounds with melting points $<-40^{\circ}$C. The minimum anion composition of these eutectics are quite high, for example $\sim$36 wt. % H_2SO_4 in the sulphuric acid-water system (Beyer 2003).

At concentrations below these values, the phase boundary between a one phase liquid state and a two phase system (solid/liquid) is set by the *liquidus* temperature curve, illustrated for the sulphuric acid-water system by Fig. 1. This curve may be used to estimate a minimum molarity for a stable liquid vein concentration above the eutectic temperature. This may be seen by considering the binary phase diagram. In Fig. 1, the region of interest is shaded. Within that region, two phases are present: ice and liquid. The ice composition is 0% sulphuric acid as determined by the tie line to the solid boundary. If a sample is cooled from any point in the liquid region to a point in the two phase region, it separates into two phases (a solid (pure H_2O ice, no sulphuric acid) and a liquid of composition defined by a tie line to the *liquidus* curve. Three example temperatures are shown in the figure: 'A' –10°C; 'B' –20°C; and 'C' –40°C. The value of the concentration at the liquid phase boundary at each temperature is approximately 16, 23 and 31 wt % H_2SO_4, respectively. The initial concentration of the liquid solution does not affect the composition of the liquid phase at that temperature. It is only controlled by the temperature and position of the *liquidus* curve. The initial composition will affect the amount of liquid produced relative to the amount of solid phase. This proportion is given by the relative length of the horizontal tie lines between the point and the *liquidus* curve on the one hand and the point and the axis on the other (a", b", and c" in Fig. 1). The ratio of the latter to the former (a":a', b":b'; c":c') gives the ratio of ice to liquid. This is known as the lever rule. The exact position of the *liquidus* line on the phase diagram is controlled by the melting point of water, the eutectic point and the chemical potential between the phases.

For an actual vein system, the thermodynamics are more complex than the simplified binary case discussed above (see, for example, Beyer and others (2004)). This is due to the fact that the existence of other constituents can alter the phase boundaries and eutectic compositions dramatically. Moreover, the width of the veins themselves and pressure within the system will contribute to the exact position of the *liquidus* curve. Still, the binary diagrams indicate that the vein concentrations may be significantly higher than those predicted by Mader and others (2006). The impact of this on vein chemistry would be profound.

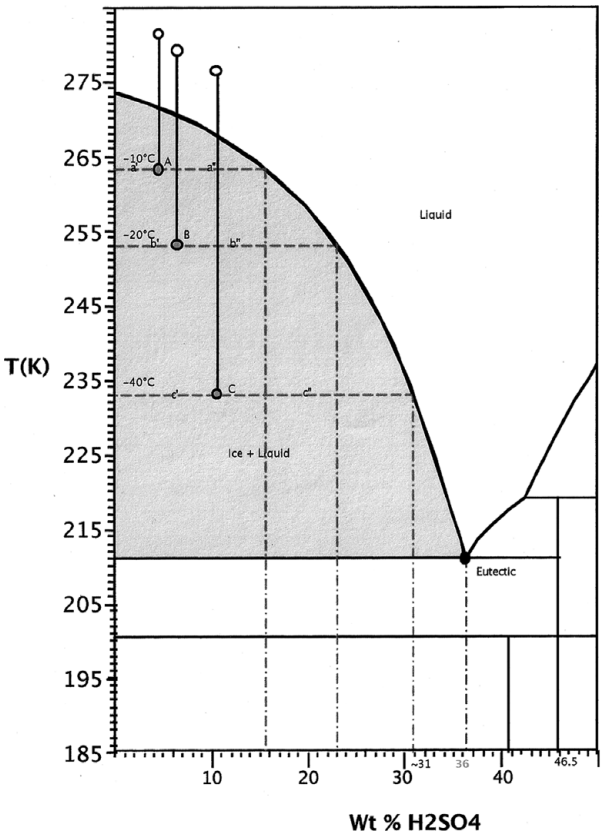

Fig. 1. Portion of binary phase diagram for the sulphuric acid–water system after Beyer and others (2003). Reprinted with permission from *Journal of Physical Chemistry A,* 107: 2025–2032(2003). Copyright (2003) American Chemical Society.

For example, based on extrapolated density data from Bump and Sibbitt (1) and the phase diagram data, one would expect a stable acid concentration for either a nitric or sulphuric acid vein systems at –15 to –20°C (Beyer 2003, 2004) to be $\sim$2.3 M. Since these concentrations cannot be predicted *a priori* due to the complexities of a multi-component system in a varying vein geometry, experimental means must be sought to directly measure the concentrations of anionic species of relevance to cryobiology. Indeed, the literature discussed above indicates that the presence of metabolising biota may themselves drastically alter the vein chemistry with respect to that determined from equilibrium considerations.

In order to remedy the deficiency in the measurement of anions of biological importance in ice veins, it is necessary to use a non-destructive analytical technique capable of high spatial resolution. Such a technique would allow for the monitoring of microbial μ-environments *in situ* as well as a more detailed understanding of extremophile metabolism and its impact in the local glacial environment. From this perspective, μ-Raman spectroscopy is a particularly useful technique. Raman spectra are produced by the inelastic scattering of a monochromatic light source. In Raman, the scattered radiation is offset from the incident laser frequency by an amount proportional

https://doi.org/10.1017/S0032247411000635 Published online by Cambridge University Press

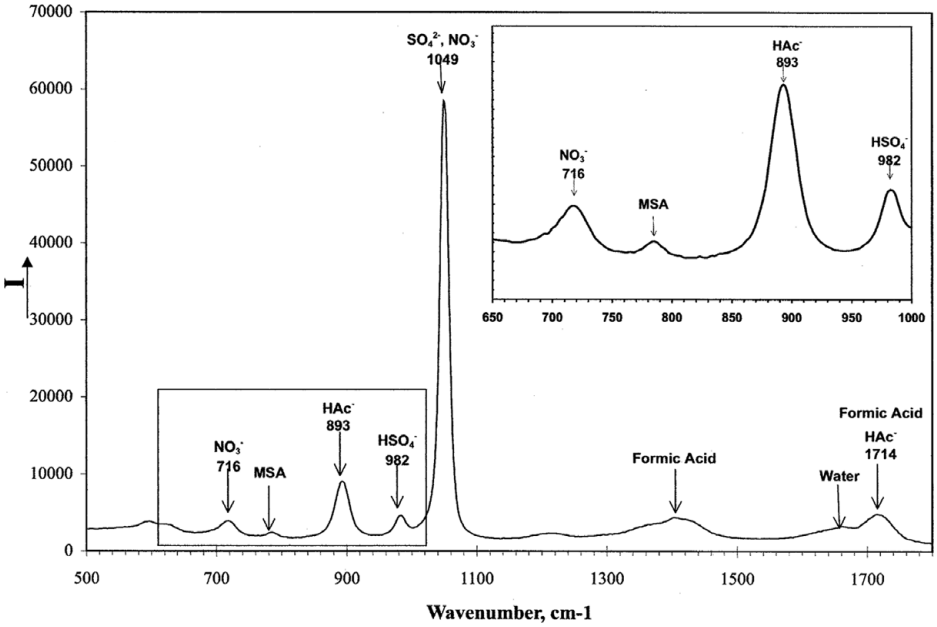

Fig. 2. Raman spectrum of Mix-1. Inset region is a magnification of region indicated on complete spectrum by the rectangle. Intensity in arbitrary units.

to the rotational or vibrational frequency of the scattering center. Thus, in Raman, a spectrum similar to an infrared spectrum can be obtained at the point of focus. Using the appropriate microscope objective, chemical information can be obtained on microscopic samples at diffraction-limited resolution. Using Raman, Barletta and others (2009) have shown that for biogenic sulphur compounds such as dimethyl sulphide (DMS) and the methane sulphonic acid anion (MSA) concentrations in the 10's of mM concentration range can be readily determined. Thus, based upon the concentration estimates of Mader and others (2006) listed in Table 1, the technique should have the requisite sensitivity.

Raman spectroscopy has found widespread application in situations in which water is a major constituent in the sample, including in marine science (Hester 2006) and the analysis of clathrates in ice-cores (Pauer 1995). This is because water is a relatively weak Raman scatterer and, in contrast to infrared spectroscopy, offers little interference in the fingerprint region. From a quantitative perspective, Barletta and others (2009) have demonstrated the efficacy of using the water bending mode as an internal standard in Raman analysis. Raman has been applied to particulate and inclusion analysis of glacial ice (see for example Sakuri 2010; Ohno 2006). However, a detailed study of the chemistry of ice veins has not been reported even though, based on the predicted concentrations of molecular anions shown in Table 1, this should be readily accomplished. This fact is illustrated in Fig. 2, which shows a Raman spectrum of a room temperature solution of the mixture defined by Mader and others (2006) given in Table 1. It can be seen from this spectrum that bands attributable to each of the anionic species can be easily identified. In order to develop the methodology for the quantification of vein chemistry using Raman spectroscopy, a series of experiments on model systems have been conducted. The results of these experiments are described below.

Experimental methods

Ice samples were prepared using solutions of single or binary components in water with variable ionic concentrations. Initial concentrations were chosen so as to be easily detectable with Raman spectroscopy. The concentrations used in this study are listed in Table 2. Ice samples were prepared by 'splat cooling' the initial solution of known concentration on either an aluminum plate or in a 33mm glass bottom culture dish with an uncoated glass window 0.085–0.13 mm thick (MatTEK P35G-0–20-C) that had been pre-cooled to –80°C by resting the aluminum block on dry ice. In the case of samples prepared on the culture dish, the dish was placed on the block. Small drops of the liquid were dropped onto the block or dish window from a distance of approximately 1.5 m. Samples prepared on the aluminum block were scraped off the block and placed in a 33 mm culture dish. A number of different solutions were studied: pure solutions of MSA^- (as NaMSA), NO_3^- (as $NaNO_3$) or SO_4^{2-}(as H_2SO_4), and mixtures of MSA with either nitrate or sulphate. Once in the culture dish, samples were annealed for 12 to 48 hours at approximately –9°C to allow for grain growth. Fig. 3 shows micrographs of typical samples containing sulphate, nitrate or MSA at 50X magnification. Table 2 lists estimated vein widths and crystal dimensions for each sample thus prepared. Crystal dimensions were determined from photographs take at 10X magnification, while vein widths were

https://doi.org/10.1017/S0032247411000635 Published online by Cambridge University Press

Table 2. Sample characteristics of splat-cooled ice samples. The number of measurements upon which the values are based are given in parenthesis. For mean crystal dimensions the number of measurements listed in the area column applies to circularity and bounding rectangle estimates as well. Uncertainties are given as 1σ.

			Microscopic characterisation				
						Mean bounding rectangle	
Species	Initial conc. (mM)	Anneal temp. (°C)	Nominal Vein Width (μm)	Mean crystal area (μm^2)	Mean circularity	Length (μm)	Width (μm)
H_2SO_4	50	9	3.3 ± 1.7 (50)	$7.0 \pm 5.1 \times 10^5$ (15)	0.7 ± 0.2	1070 ± 530	930 ± 420
	75	9	3.1 ± 1.7 (66)	$3.3 \pm 3.1 \times 10^5$ (15)	0.82 ± 0.6	620 ± 330	610 ± 330
$NaNO_3$	31	9	2.7 ± 1 (50)	$1.8 \pm 2.0 \times 10^5$ (33)	0.8 ± 0.1	470 ± 290	460 ± 230
	55	9	2.2 ± 0.6 (50)	$2.1 \pm 2.0 \times 10^5$ (26)	0.7 ± 0.2	500 ± 240	500 ± 280
	200	9	2.8 ± 1.2 (23)	$4.8 \pm 2.4 \times 10^5$ (9)	0.84 ± 0.07	860 ± 260	760 ± 250
NaMSA	10	9	2.9 ± 1.2 (50)	$9.0 \pm 6.8 \times 10^4$ (31)	0.83 ± 0.06	360 ± 150	340 ± 120
	21	9	1.2 ± 0.3 (50)	$8.1 \pm 8.5 \times 10^4$ (83)	0.85 ± 0.04	330 ± 150	310 ± 130
	55	9	1.7 ± 1.0 (50)	$1.0 \pm 0.8 \times 10^5$ (55)	0.82 ± 0.07	360 ± 150	360 ± 140
Mixture 1							
NaMSA	58	9	8.2 ± 3.6 (55)	$1.5 \pm 1.3 \times 10^5$ (32)	0.79 ± 0.11	460 ± 220	435 ± 190
H_2SO_4	52						
Mixture 2							
NaMSA	51	9	3.1 ± 1.1 (39)	$1.6 \pm 1.7 \times 10^5$ (34)	0.71 ± 0.12	470 ± 310	420 ± 220
$NaNO_3$	55						

estimated from 50X micrographs such as those shown in Fig. 3. All measurements were made using NIH ImageJ. Crystal sizes were measured using two means: area of the crystal as determined by an irregular polygon fit and dimensions of a rectangle enclosing the crystal. In addition, for each area measurement, the degree of circularity was also estimated.

Once annealed, the culture dish containing the ice sample was placed on a cooled microscope stage. Raman spectra were taken of both bulk ice crystals and ice veins/vein triple junctions and liquid inclusions at multiple locations. Using a μ-Raman system previously described, equipped with a 488 nm Ar-ion laser as an excitation source, typical spectra were taken at approximately –15°C by summing ten one-second scans. The laser power was measured incident to the microscope and absorption by microscope optical elements corrected for to estimate the incident laser power at the sample. Table 3 lists the measurement conditions for all samples studied. Fig. 4 shows a typical spectrum for a vein sample prepared using 10 mM MSA^- solution along with the Raman spectrum of the as-prepared solution. Fig. 5 shows a typical spectrum for a vein sample prepared using 50 mM H_2SO_4 solution along with the Raman spectrum of the as-prepared solution. Finally, Fig. 6 shows a typical spectrum for a vein sample prepared using 31 mM NO_3^- solution along with the Raman spectrum of the as-prepared solution.

Results and discussion

From a consideration of relative peak heights in Figs. 3 to 6, it can be seen that the concentration of the various anions in ice veins increases relative to the initial solution concentration. Quantitative estimates of the concentrations of MSA, sulphate and nitrate anions in the veins were determined by band fitting of Raman spectrum using Gaussian peaks in the region of interest with the peak fitting routine available in GramsAI™. The band areas of the characteristic bands of the anionic species thus obtained were normalised to the Raman band associated with water bending mode at ~1640 cm^{-1}. These relative peak heights were then used to calculate the concentration of the anion by using a calibration curve prepared with standard solutions in a method similar to that described by Barletta and others (2009). For MSA, two bands could be used to obtain the sample concentration, that is the C-S stretching mode at ~787 cm^{-1} and the S-O stretching mode at ~1051 cm^{-1}. The agreement between these two modes was quite good. For nitrate, the strong band at ~1044 cm^{-1} was used to determine the concentration (Ianoul 2002). For sulphate, the situation is a more complicated as the two strongest bands are associated with two different species, the HSO_4^- (~1050 cm^{-1}) and SO_4^{2-} (~981 cm^{-1}) ions (Irish 1970). The total concentration of sulphate is determined from the sum of these two contributions. The calibration curve was prepared from a known amount of sulphuric acid and the concentration of sulphate and bisulphate was calculated using the temperature corrected equilibrium constant. Table 3 gives the calculated concentration for each species measured in the vein samples

For measurements made on the interior of the crystals themselves, bands attributable to the anionic species of interest (nitrate, sulphate, bisulphate, or MSA anions) were either absent or barely detectable. Further, as illustrated in Figs. 3 to 6, well known shifts in intensity, position and band shape of the bending mode of water

https://doi.org/10.1017/S0032247411000635 Published online by Cambridge University Press

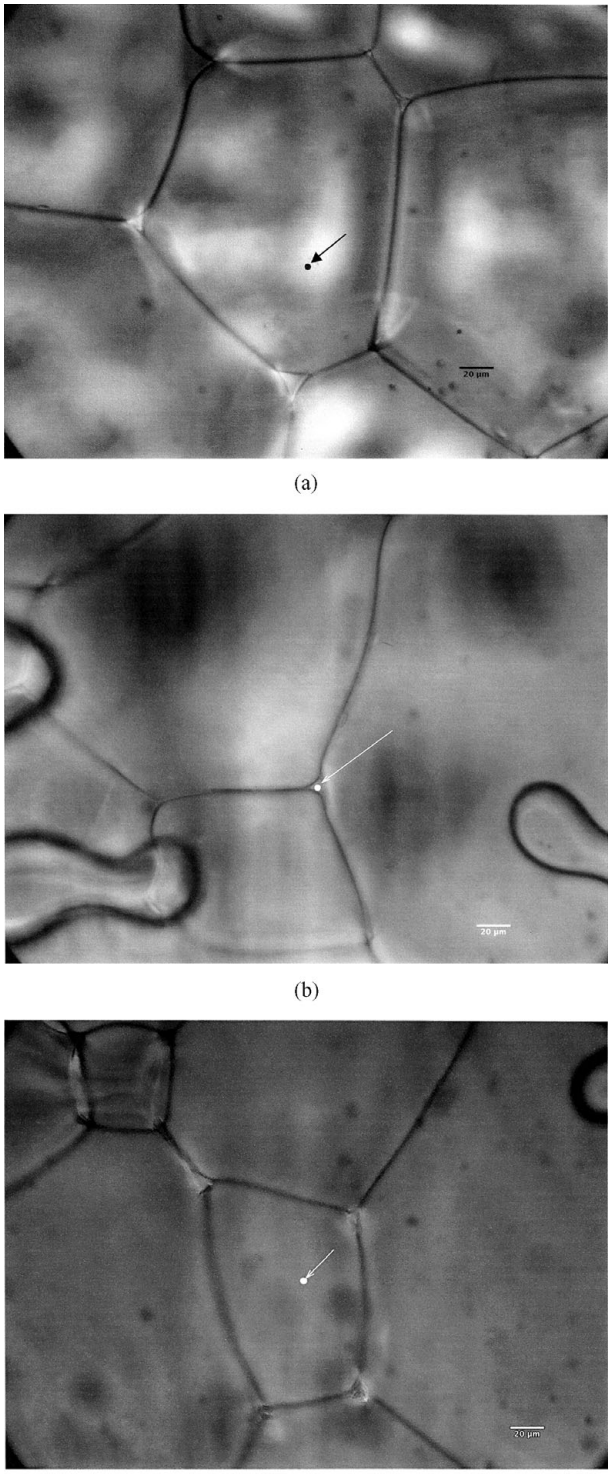

Fig. 3. Typical sample of splat cooled, annealed ice samples (50X). Dot indicates region of analysis. (Note: Irregular forms are gas bubbles/voids in sample.) (a) Sulfate ice – initial solution concentration 50mM H_2SO_4; (b) Nitrate ice - initial solution concentration 55mM $NaNO_3$; (c) MSA ice - initial solution concentration 55mM NaMSA.

upon freezing (Kanno 1998) were observed. This fact alone made quantification using band ratios to the water bending mode impossible as the calibration curve prepared for solution spectra was not applicable. Since some sublimation of the sample undoubtedly occurred during annealing, it is possible that trace amounts of solids were present on the surface. Surface contaminiation would account for the presence of bands attributable to the anionic species of interest. However, particulates were not observed in the region of ice crystals selected for analysis. On the whole, analysis of the ice crystals as opposed to ice veins are consistent with the conclusion that the anions are excluded from the ice lattice during freezing (Mader 2006).

From a quantitative perspective, the analysis of the concentrations in the ice veins themselves is another matter. Mader and others (2006) predict that vein concentrations in glacial ice should be quite high, that is on the order of those observed in these experiments. It must be noted that the initial concentrations used in these experiments are some three orders of magnitude higher than the corresponding anion concentrations in glacial ice. Initial concentrations in this range were chosen for these experiments in order to be above the minimum detection limits for these anions in solution by Raman analysis (~10 mM). Even given the concentration range used to prepare the ice samples, the data in Table 3 for maximum vein concentration do not show a strong correlation with the initial solution concentration even when the latter is varied over almost a full order of magnitude. Given the equilibrium phase diagram discussions above, which imply the vein concentration does not depend on the initial solution concentration as long as it is below the eutectic concentration of the species, this is not surprising. It is possible that the maximum concentrations given in Table 3 may represent a better estimate of the vein concentrations, as the minimum concentrations measured in veins may be indicative of inclusion of crystalline ice in the volume sampled by the laser beam, thus reducing the observed concentration. From a thermodynamic perspective, there should be a minimum concentration in the vein representing the position of the *liquidus* curve. However, as discussed above, this may not correspond to that implied by the *liquidus* curve defined by bulk measurements of binary mixtures at atmospheric pressure.

In spite of the potential to underestimate the concentration and the large variability seen in the concentration measurements listed in Table 3, the mean vein concentration measurements observed appear to be reasonable estimates of the anionic concentrations in the vein. This was verified by using these values to calculate the initial solution concentration and comparing this calculated value with the actual solution concentration. The methodology for calculating the initial concentration from the vein concentration involves determining the fractional vein volume and multiplying the mean concentration by this value. This approach was similar to

https://doi.org/10.1017/S0032247411000635 Published online by Cambridge University Press

Table 3. Analysis conditions and calculated vein concentrations for splat-cooled samples. Uncertainties are given as 1σ. For average concentrations, these uncertainties represent standard deviation of all measurements, while for maximum and minimum values they are determined using the uncertainties in the least squares fit of the calibration curve. nm = power not recorded, however, it is estimated to be in the range of 75 to 150 mW.

		Analysis conditions				Raman analysis		
Species	Initial Conc. (mM)	Analysis temp. (°C)	Avg. power @ sample (mW)	No. of veins meas.	No. of crystals meas.	Mean Vein Conc. (mM)	Max. Vein Conc. (mM)	Min. Vein Conc. (mM)
H_2SO_4	50	−15	69 ± 7	13	3	230 ± 110[a]	480 ± 10[a]	60 ± 10[a]
	75	−15	nm	5	3	3530 ± 330[a]	4110 ± 70[a]	3130 ± 60[a]
$NaNO_3$	31	−15	109 ± 1	10	5	540 ± 410	1220 ± 10	56 ± 1
	55	−17 ± 1	154 ± 2	10	0	710 ± 480	1280 ± 9	135 ± 1
	200	−15	nm	8	6	1280 ± 140	1400 ± 10	1012 ± 7
NaMSA	10	−15	nm	4	2	876 ± 240[b]	1070 ± 50[b]	530 ± 30[b]
						830 ± 230[c]	1000 ± 10[c]	490 ± 1[c]
	21	−15	65 ± 4	14	4	690 ± 33[b]	1200 ± 60[b]	340 ± 20[b]
						630 ± 32[c]	1130 ± 10[c]	259 ± 3[c]
	55	−15	69 ± 6	14	4	1670 ± 130[b]	1810 ± 90[b]	1300 ± 70[b]
						1600 ± 120[c]	1730 ± 20[c]	1200 ± 20[c]
Mixture 1								
NaMSA	58	−15	77 ± 2	11	2	450 ± 200[b]	700 ± 40[b]	130 ± 10[b]
H_2SO_4	52					2160 ± 120[a]	3470 ± 140[a]	59 ± 4[a]
Mixture 2								
NaMSA	51	−15	77 ± 20	7	3	780 ± 70[b]	840 ± 40[b]	680 ± 40[b]
$NaNO_3$	55					1220 ± 110	1340 ± 10	1050 ± 10

[a]sum of sulphate anion concentration plus bisulphate anion concentration; [b]based on C-S stretch; [c]based on S-O stretch

that used by Ohno and others (2006) in calculating μ-inclusion contributions to ion content in glacial ice. If the ice film is uniform in thickness, the fractional volume can be determined from the ratio of vein area to total area in a fixed area on a micrograph. When this was done for all the three MSA samples, reasonable agreement between the initial concentration and that calculated from the mean vein concentration was obtained. For MSA initial solution concentrations ranging from 10 to 55 mM, the initial concentration could be determined from the mean vein within 9 to 20%. This is about the same degree of variation in the mean concentration of vein MSA listed in Table 3. The implication of this result is that this method has the potential to non-destructively estimate bulk ice concentrations

More importantly, from the standpoint of assessing the biological impacts of vein chemistry, these results enable a direct measurement of vein pH from acidic species. This can be seen from results of samples prepared from sulphuric acid. In a sulphuric acid solution, the pH of the solution is determined by the K_a of the second dissociation:

$$HSO_4^- \quad \rightarrow \quad H^+ + SO_4^{2-}$$

along with the ratio of the sulphate to bisulphate concentration. For the sulphate/bisulphate system, K_a has been determined as a function of temperature (Knopf 2003). Using the sulphate and bisulphate concentrations measured in the vein samples for both the 75 mM sulphate and the mixture 2 (sulphate/MSA mixture, 52 mM sulfate) splat-cooled ice, a pH of 1.0 ± 0.1 over a total of 16 measurements was calculated. For the 50mM solution, the estimated pH is much higher, 2.2 ± 0.3, although still quite acidic. By comparison, the calculated pH's in ice veins are much lower than that estimated from deep sea hydrothermal vents (<3) (Reysenbach 2006). Should such levels of pH exist in glacial ice veins, the ice vein μ-habitat could be considered truly extreme.

A final observation on the splat-cooled specimens is somewhat puzzling. For the two mixtures studied, it was found that both the nitrate and sulphate components were enriched in the vein relative to the MSA when compared to the concentration in the original solution. For the MSA sulphate mixture, this increase in concentration was slightly over a factor of five. Such an increase could be qualitatively explained by the precipitation of solid MSA in preference to its incorporation into the vein fluid. The precipitation of a MSA salt would be consistent with the presence of MSA micro-particles found in Fuji Dome ice, as well as the fact the a relatively high temperature eutectic [$(CH_3SO_3)_2Mg{\cdot}nH_2O$, m.p. = −5°C)] is known (Sakurai 2010). However, it should be noted that large amounts of particulate were not observed in or around the veins in the mixtures studied. It may be that, for our

https://doi.org/10.1017/S0032247411000635 Published online by Cambridge University Press

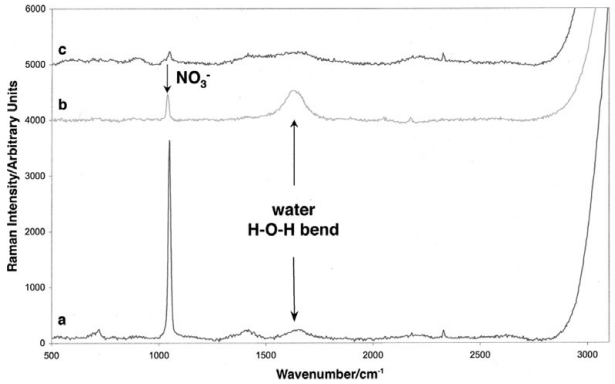

Fig. 4. Typical vein Raman spectrum for splat-cooled 31 mM nitrate at −15.1°C along with a reference Raman spectrum for initial aqueous solution at room temperature. The Raman spectrum of a typical crystal is shown for comparison. The calculated nitrate vein concentration was 788 mM. Spectra baselined to remove Petri dish background and offset for clarity. (a) vein spectrum; (b) solution spectrum; (c) ice crystal.

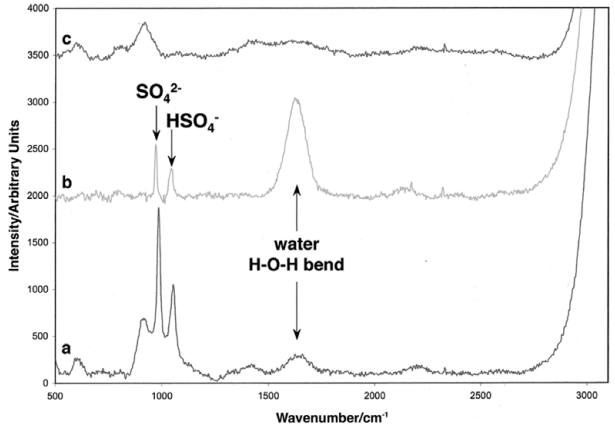

Fig. 5. Typical vein Raman spectrum for splat-cooled 50 mM sulfuric acid at −15.0°C along with a reference Raman spectrum for initial aqueous solution at room temperature. The Raman spectrum of a typical crystal is shown for comparison. The calculated H_2SO_4 vein concentration was 266 mM, based on summing sulfate (204mM) and bisulfate (62 mM) contributions. Spectra baselined to remove Petri dish background and offset for clarity. (a) vein spectrum; (b) solution spectrum; (c) crystal spectrum.

samples, the particle size of any solid MSA was much less than the microscope resolution (<1 μm) due to the sample preparation method and, in this case, the presence of such small particles cannot be confirmed even though our annealing and measurement temperature was much lower than the eutectic melting point.

Conclusions

This study demonstrates the usefulness of μ-Raman spectroscopy as a tool for quantitative measurement of

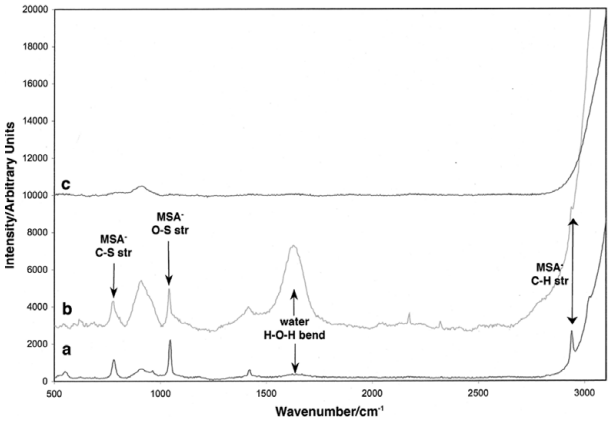

Fig. 6. Typical vein Raman spectrum for splat-cooled 21mM MSA at −14.9°C along with a reference Raman spectrum for initial aqueous solution at room temperature. The Raman spectrum of a typical crystal is shown for comparison. The calculated MSA^- vein concentration 675 mM, based on averaging estimates derived from using the C-S and SO stretching modes. Spectra baselined to remove Petri dish background and offset for clarity. (a) vein spectrum; (b) solution spectrum; (c) ice crystal spectrum.

molecular ion concentration in ice veins. As such, it has great applicability in the area of nondestructive analysis of both glacial and sea ice samples. This is important in those instances in which sample volume conservation is important. Ohno and others (2005) have noted that the fraction of these ions trapped in vein liquids may vary considerably, but this work, along with their studies on inclusion composition (Ohno and others 2005, 2006; Sakuri 2010) offer a path forward to determining the relative contributions of inclusion and vein sequestration of impurities in ice as well as the factors which control partitioning in a particular sample. A complementary technique to obtain cation concentration nondestructively would be of particular value in this regard.

This work further demonstrates the variability present in ice vein composition. This variability is, in part controlled by both ice crystal and vein dimensions that are themselves functions of variables such as temperature, annealing time, and pressure (Mader 1992). From this perspective the model systems studied in this work are not directly applicable to natural systems, especially given the fact that the bulk concentrations of the anions used in this study are orders of magnitude greater than those found in glacial ice. However, it must be noted that, based upon the particulars of phase relationships discussed in the introduction, the bulk concentration may not have a large contribution to the determination of the anion concentration present in the liquid phases in glacial ice

From the standpoint of understanding ice veins as μ-habitats in closed systems, the results obtained from the model systems studied are of great relevance. To the

https://doi.org/10.1017/S0032247411000635 Published online by Cambridge University Press

extent sulphate exists as an acidic medium in these veins, it may be concluded that extremely low pH values are likely present. Moreover, regardless of the pH, the overall ionic strength of vein solutions is extremely high. The impact of microbes on this chemistry was not explicitly addressed in this study, but the techniques employed in this work should enable this information to be obtained. Further, given the non-destructive nature of this approach, it may be possible to directly measure metabolic rates of extremophiles contained in ice samples. Future work on ice containing trapped microbes and algae is planned in order to explore this possibility.

Acknowledgements

This study was funded by the National Science Foundation, Office of Polar Programs under Grant No. 0828786. The authors would like to acknowledge the contributions of Dr. Heidy Mader, for her many helpful technical discussions and suggestions concerning the manuscript.

References

Barletta, R.E., B.N. Gros, and M.P. Herring. 2009. Analysis of marine biogenic sulfur compounds using Raman spectroscopy: dimethyl sulfide and methane sulfonic acid. *Journal of Raman Spectroscopy* 40: 972–981.

Beyer, K.D., and A.R. Hansen. 2002. Phase diagram of the nitric acid/water system: implications for polar stratospheric clouds. *Journal of Physical Chemistry* A 106: 10275–10284.

Beyer, K.D., A.R. Hansen, and M. Poston. 2003. The search for sulfuric acid octahydrate: experimental evidence. *Journal of Physical Chemistry* A 107: 2025–2032.

Beyer, K.D., A.R Hansen, and N. Raddatz. 2004. Experimental determination of the $H_2SO_4/HNO_3/H_2O$ phase diagram in regions of stratospheric importance. *Journal of Physical Chemistry* A 108: 770–778.

Bump, T.R., and W.L. Sibbitt. 1955. Heat transfer design data - aqueous solutions of nitric acid and of sulfuric acid. *Industrial Engineering Chemistry* 47(8): 1665–1670.

Christner, B.C. 2010. Bioprospecting for microbial products that affect ice crystal formation and growth. *Applied Microbiology and Biotechnology* 85: 481–489.

Eichen, H. 1992. The role of sea ice in structuring Antarctic ecosystems. *Polar Biology* 12: 3–13.

Hester, K.C., S.N. White, E.T. Peltzer, P.G. Brewer, and E.D. Sloan. 2006. Raman spectroscopic measurements of synthetic gas hydrates in the ocean. *Marine Chemistry* 98: 304–314.

Ianoul, A., T. Coleman, and S.A. Asher. 2002. UV resonance Raman spectroscopic detection of nitrate and nitrite in wastewater treatment processes. *Analytical Chemistry* 74(6): 1458–1461.

Irish, D.E., and H. Chen. 1970. Equilibria and proton transfer in the bisulfate-sulfate system. *Journal of Physical Chemistry* 74(24): 3796–3801.

Kanno, H., K. Tomikawa, and O. Mishima. 1998. Raman spectra of low- and high-density amorphous ices. *Chemical Physics Letters* 293: 412–416.

Knopf, D.A., B.P. Luo, U.K. Krieger, and T. Koop. 2003. Thermodynamic dissociation constant of the bisulfate ion from Raman and ion interaction modeling studies of aqueous sulfuric acid at low temperatures. *Journal of Physical Chemistry* A 107: 4322–4332.

Mader, H.M. 1992. The thermal behaviour of the water-vein system in polycrystalline ice. *Journal of Glaciology* 38: 359–374.

Mader, H.M., M.E. Pettitt, J.L. Wadham, E.W. Wolff, and R.J. Parkes. 2006. Subsurface ice as a microbial habitat. *Geology* 34: 169–172.

Ohno, H., M. Igarashi, and T. Hondoh. 2005. Characteristics of salt inclusions in polar ice from Dome Fuji, East Antarctica. *Geophysical Research Letters* 33: L0850.

Ohno, H., M. Igarashi, and T. Hondoh. 2006. Salt inclusions in polar ice core: location and chemical form of water-soluble impurities. *Earth and Planetary Sciences Letters* 232: 171–178.

Pauer, F., J. Kipfstuhl, and W.F. Kuhs. 1995. Raman spectroscopic study on the nitrogen/oxygen ratio in natural ice clathrates in the GRIP ice core. *Geophysical Research Letters* 22: 969–971.

Price, B.P. 2009. Material genesis, life and death in glacial ice. *Canadian Journal of Microbiology* 55: 1–11.

Priscu, J.C., B.C. Christner, C.F. Foreman, and G. Royston-Bishop. 2007. Biological material in ice cores. *Encyclopedia of Quaternary Science* 2: 1156–1166.

Rohde, R.A., and P.B. Price. 2006. Diffusion-controlled metabolism for long-term survival of single isolated microorganisms trapped within ice crystals. *Proceedings of the National Academy of Science* 104: 16592–16597.

Rohde, R.A, P.B. Price, R.C. Bay, and N.E. Bramall 2008. *In situ* microbial metabolism as a cause of gas anomalies in ice. *Proceedings of the National Academy of Science* 105: 8667–8672.

Reysenbach, A., Y. Liu, A.B. Banta, T.J. Beveridge, J.D. Kirshtein, S. Schouten, M.K. Tivey, K.L. Von Damm, and M.A. Voytek. 2006. A ubiquitous thermoacidophilic archaeon from deep-sea hydrothermal vents. *Nature* 442: 444–447

Sakurai, T., H. Ohno, F.E. Genceli, S. Horikawa, Y. Iizuka, T. Uchida, and T. Hondoh. 2010. Magnesium methanesulfonate salt found in the Dome Fuji (Antarctica) ice core. *Journal of Glaciology* 56: 837–842.

Stevens, J. 1995. The Antarctic pack-ice ecosystem. *BioScience* 45(3): 128–132.

Thomas, D.N., and G.S. Dieckmann. 2002. Antarctic sea ice – a habitat for extremeophiles. *Science* 295: 641–644.

Tung, H.C., P.B. Price, N.E. Bramall, and G. Vrdoljak. 2006. Microorganisms metabolizing on clay grains in 3-km-deep Greenland basal ice. *Astrobiology* 6: 69–86.